

Mesenchymal Multipotency of Adult Human Periosteal Cells Demonstrated by Single-Cell Lineage Analysis

Cosimo De Bari,¹ Francesco Dell'Accio,¹ Johan Vanlauwe,² Jeroen Eyckmans,² Ilyas M. Khan,³ Charles W. Archer,³ Elena A. Jones,⁴ Dennis McGonagle,⁴ Thimios A. Mitsiadis,¹ Costantino Pitzalis,¹ and Frank P. Luyten²

Objective. To investigate whether periosteal cells from adult humans have features of multipotent mesenchymal stem cells (MSCs) at the single-cell level.

Methods. Cell populations were enzymatically released from the periosteum of the proximal tibia obtained from adult human donors and then expanded in monolayer. Single-cell-derived clonal populations were obtained by limiting dilution. Culture-expanded periosteal cell populations were tested for their growth potential and for expression of conventional markers of MSCs and were subjected to *in vitro* assays to investigate their multilineage potential. To assess their multipotency *in vivo*, periosteal cells were injected into a regenerating mouse tibialis anterior muscle for skeletal myogenesis or were either seeded into an osteoinductive matrix and implanted subcutaneously into nude mice for osteogenesis or implanted in a joint surface defect under a periosteal flap into goats for chondrogenesis. Cell phenotypes were analyzed by histochemistry and immunohistochemistry and by reverse transcription–polymerase chain reaction for the expression of lineage-related marker genes.

Results. Regardless of donor age, periosteal cells were clonogenic and could be expanded extensively in monolayer, maintaining linear growth curves over at least 30 population doublings. They displayed long telomeres and expressed markers of MSCs. Under specific conditions, both parental and single-cell-derived clonal cell populations differentiated to the chondrocyte, osteoblast, adipocyte, and skeletal myocyte lineages *in vitro* and *in vivo*.

Conclusion. Our study demonstrates that, regardless of donor age, the adult human periosteum contains cells that, upon enzymatic release and culture expansion, are multipotent MSCs at the single-cell level.

Joint destruction represents the consequence of most inflammatory and degenerative rheumatic diseases and results from a failure of reparative processes to counteract the tissue damage induced by injuring factors. So far, a great effort has been made to develop therapeutic approaches aimed at removing/controlling inflammation, but few therapeutic approaches are available for modulating repair. In addition, patients with late-stage diseases are often seen in daily practice in rheumatology, when the tissue damage is already established. Under these circumstances, skeletal tissue repair represents an important therapeutic goal.

Regenerative medicine presents the opportunity not only to control the progression of diseases, but also to promote repair through tissue regeneration. One strategy is the use of mesenchymal stem cells (MSCs), which are clonogenic undifferentiated cells that, at the single-cell level, are capable of both self-renewal and differentiation into lineages of mesenchymal tissues, including cartilage, bone, adipose tissue, and skeletal muscle. The “conventional” MSCs are those obtained from bone marrow (1–3). However, MSCs have been isolated from several other tissues as well (4–12).

Supported by FWO grant G.0192.99 and by IWT grant 000259. Dr. De Bari is a Fellow of the Medical Research Council, UK. Dr. Dell'Accio is a Fellow of the Arthritis Research Campaign, UK.

¹Cosimo De Bari, MD, PhD, Francesco Dell'Accio, MD, PhD, Thimios A. Mitsiadis, DDS, PhD, HDR, Costantino Pitzalis, MD, PhD, FRCP: King's College London, London, UK; ²Johan Vanlauwe, MD, Jeroen Eyckmans, Frank P. Luyten, MD, PhD: University Hospitals, Katholieke Universiteit Leuven, Leuven, Belgium; ³Ilyas M. Khan, PhD, Charles W. Archer, PhD: Cardiff University, Cardiff, UK; ⁴Elena A. Jones, PhD, Dennis McGonagle, PhD, FRCPI: University of Leeds, Leeds, UK, and Calderdale Royal Hospital, Halifax, UK.

Address correspondence and reprint requests to Cosimo De Bari, MD, PhD, Department of Rheumatology, King's College London School of Medicine, Thomas Guy House, Floor 5, Guy's Hospital, London SE1 9RT, UK. E-mail: cosimo.debari@kcl.ac.uk.

Submitted for publication August 24, 2005; accepted in revised form January 5, 2006.

Periosteum-derived cell preparations can form cartilage and bone *in vitro* and *in vivo* (13–21) as well as adipocytes *in vitro* (22) and, therefore, have been used in tissue engineering protocols (23–26). However, it is not known whether the capacity of periosteum-derived cell populations to form multiple tissues is due to the presence of a cell type with inherent mesenchymal multipotency or to the coexistence of functionally distinct progenitor cell types, each with a specific differentiation potential, as suggested by a previous *in vitro* study (27). Indeed, periosteum is at the boundary between the bone and the surrounding soft tissues and contains multiple cell types (e.g., cells of the cambium layer, fibrous layer, blood vessels, and pericytes) that could potentially function as progenitor cells. This issue has important implications in the preparation of cellular products for clinical applications. Indeed, an important challenge in cell-based therapies is to obtain cell preparations with a reproducible behavior in terms of tissue formation.

The strategy for obtaining cell populations with predictable tissue formation capacity would be dependent, at least in part, on the presence of either multiple functionally distinct cell subsets or more primitive stem cells capable of multilineage differentiation. In the former case, the strategy would focus on the identification and separation of the cell subset with the desired tissue-forming capacity from cell subpopulations with unwanted differentiation potential(s); in the latter case, cell product manufacturing, including culture techniques, scaffold technologies, or growth factor treatments, could be pivotal in the commitment to the desired tissue(s) and/or in the prevention of unwanted/heterotopic tissue formation.

In the present study, we characterized the growth potential and phenotype of adult human periosteal cell populations and investigated the presence of multipotent clonogenic cells by performing single-cell lineage analysis.

MATERIALS AND METHODS

Isolation and culture of periosteal cells. Samples of periosteum measuring 1 cm² were harvested aseptically from the proximal medial tibia of 12 human donors (median age 54 years [range 24–83 years]); samples were obtained either postmortem (within 12 hours after death) or at the time of surgical knee replacement because of degenerative osteoarthritis. Cells were isolated and expanded in monolayer on plastic and in growth medium (high-glucose Dulbecco's modified Eagle's medium [Life Technologies, Paisley, UK] containing 10% fetal bovine serum [selected lot from Life Technolo-

gies] and antibiotics [Life Technologies]), as described previously (19). Except for the cell cloning, all experiments were performed with expanded cell populations between passages 3 and 10.

Cloning of periosteal cells. Cell cloning was performed by limiting dilution. First-passage periosteal cells were suspended in growth medium and plated at a density of 0.5 cells/well in 96-well flat-bottomed culture plates. At this density, the probability that clonal populations would derive from 1 single cell, as calculated by Poisson statistics, is nearly 95% (28). Cell populations arising from single cells were subcultured with serial 1:4 dilution passages upon reaching confluence. Seven expandable clones were obtained from 4 different donors.

Determination of telomerase activity. Telomerase activity was determined semiquantitatively in passage 5 periosteal cells by the telomerase polymerase chain reaction (PCR) enzyme-linked immunosorbent assay (ELISA) kit (Roche, Lewes, UK), as described previously (4). Absorbance was measured at 450 nm, with a reference wavelength of 690 nm. Samples were regarded as telomerase positive when the difference in absorbance was $>0.2 A_{450\text{ nm}} - A_{690\text{ nm}}$ units. Human dermal fibroblasts and human embryonic kidney 293 cells were used as cell negative and positive controls, respectively. For a telomerase-negative control, the 293 cell lysate was heat-treated prior to the reaction.

Telomere length assay. Genomic DNA was extracted from passage 7 periosteal MSC (Pe-MS) monolayers using standard protocol. Telomere lengths were determined semiquantitatively by Southern blotting using a TeloTAGGG Telomere Length Assay (Roche) according to the manufacturer's protocol.

Phenotyping of culture-expanded Pe-MSCs using 3-color flow cytometry. Culture-expanded (passages 4–6) Pe-MSCs were used for flow cytometry at 10⁵ cells/test. Test antibodies were as follows: phycoerythrin (PE)-conjugated low-affinity nerve growth factor receptor (LNGFR)/p75, CD106/vascular cell adhesion molecule 1, CD146/MUC18, CD166/activated leukocyte cell adhesion molecule, CD73/SH3 (all from PharMingen, Oxford, UK), CD105/SH2 (Serotec, Oxford, UK), fluorescein isothiocyanate (FITC)-conjugated CD45 (Dako, High Wycombe, UK), and CD13 (Serotec). D7-FIB-PE was labeled in-house from purified D7-FIB (Serotec). Hybridoma cells B4-78 against bone and liver isoforms of alkaline phosphatase were obtained from the Developmental Studies Hybridoma Bank of the University of Iowa (Iowa City, IA). Hybridoma supernatant was produced in-house, and antibody labeling was detected using secondary goat anti-mouse FITC (Serotec). Isotype-specific negative control antibodies were purchased from Serotec. Dead cells were gated out based on propidium iodide exclusion (Sigma, Poole, UK). All flow cytometry data were analyzed with WinMDI version 8 software (Scripps Research Institute, La Jolla, CA).

Assessment of *in vitro* adipogenesis. The *in vitro* adipogenesis assay was performed as described previously (4). Human dermal fibroblasts were used as a cell negative control. After 3 weeks, cells were rinsed with phosphate buffered saline (PBS), fixed with 0.2% glutaraldehyde (Sigma), stained with oil red O (0.1% oil red O [Sigma] in 60% isopropanol), and counterstained with hematoxylin, as described previously (4).

Table 1. Primers used for RT-PCR analysis and expected sizes of PCR products*

Gene	Primer sequence	Amplicon, bp
mh- β -actin	Forward: 5'-TGACGGGGTCACCCACACTGTGCCCATCTA-3' Reverse: 5'-CTAGAAGCATTTCGGGTGGACGATGGAGGG-3'	661
h- β -actin	Forward: 5'-CCGACAGGATGCAGAAGGAG-3' Reverse: 5'-GGCACGAAGGCTCATCATTC-3'	662
aP2	Forward: 5'-TATGAAAGAAGTAGGAGTGGGC-3' Reverse: 5'-CCACCACAGTTTATCATCCTC-3'	290
h-MyHC-IIx/d	Forward: 5'-ATAGGAACACCCAAGCCATC-3' Reverse: 5'-TTTGCCTAGACCCTTGACAG-3'	599
BMP-2	Forward: 5'-CAGAGACCCACCCCGAGCA-3' Reverse: 5'-CTGTTTGTGTTTGGCTTGAC-3'	672
α 1(II) collagen	Forward: 5'-CCCTGAGTGGAAAGAGTGGAG-3' Reverse: 5'-GAGGCGTGAGGTCTTCTGTG-3'	511
FGFR-3	Forward: 5'-GCTGAAAGACGATGCCACTG-3' Reverse: 5'-AGGACCCCAAAGGACCAGC-3'	522
GDF-5/CDMP-1	Forward: 5'-GCCCTGTTCCCTGGTGTGG-3' Reverse: 5'-GCTGTGTAGATGCTCCTGCC-3'	595
h- β -actin†	Forward: 5'-CACGGCTGCTTCCAGCTC-3' Reverse: 5'-CACAGGACTCCATGCCAG-3'	134
h-osteopontin†	Forward: 5'-GCCGACCAAGGAAAACACTCACTA-3' Reverse: 5'-CAGAAGTCCAGAAATCAGCCTGTT-3'	106
h-osteocalcin†	Forward: 5'-CCTCACACTCCTCGCCTATT-3' Reverse: 5'-CCCTCCTGCTTGGACACAAA-3'	117
h-BSP†	Forward: 5'-AAACGAAGAAAGCGAAGCAGAA-3' Reverse: 5'-GCTGCCGTTGCCGTTTT-3'	94

* The prefix "h-" means that the primer set allows specific amplification of the human cDNA. The prefix "mh-" means that the primer set does not allow a distinction between mouse and human cDNA. RT-PCR = reverse transcription-polymerase chain reaction; aP2 = an adipocyte marker; MyHC-IIx/d = myosin heavy-chain type IIx/d; BMP-2 = bone morphogenetic protein 2; FGFR-3 = fibroblast growth factor receptor 3; GDF-5/CDMP-1 = growth differentiation factor 5/cartilage-derived morphogenetic protein 1; BSP = bone sialoprotein.

† Primer used for quantitative RT-PCR.

For quantitation, the number of oil red-positive cells was calculated as a percentage of the total cells.

Adenovirus transduction. The replication-deficient recombinant adenovirus containing the *LacZ* gene under the transcriptional control of the cytomegalovirus (CMV) promoter (AdCMVLacZ) and the empty backbone adenovirus were gifts from the Center for Transgene Technology and Gene Therapy (Leuven, Belgium). For transduction, cells were replated in growth medium after addition of the virus at 10 multiplicities of infection. The next day, the virus supernatant was removed, and the cells were washed with several changes of medium. Five days later, cells were harvested for the in vivo myogenesis assay. The efficiency of transduction was ~40%.

In vivo myogenesis. Animal experimentation protocols were approved by the local ethics committee. Eight-week-old female NMRI *nu*^{-/-} mice were used for the in vivo model of muscle regeneration as described elsewhere (7). Briefly, 25 μ l of 10 μ M cardiotoxin (Latoxan, Valence, France) was injected into the tibialis anterior muscle. The next day, 5 \times 10⁵ periosteal cells suspended in 25 μ l of PBS was administered into the same tibialis anterior muscle. After 3–4 weeks, mice were killed by cervical dislocation, and their tibialis anterior muscles were excised. For total RNA extraction, tibialis anterior muscles were homogenized in TRIzol (Life Technologies). Whole-mount X-Gal staining of tibialis anterior muscles was performed overnight at 30°C according to the standard method. Muscles were then embedded in paraffin and

sectioned at 7 μ m to observe *LacZ* expression at the cellular level.

In vitro chondrogenesis. The in vitro chondrogenesis assay, which consists of a combination of micromass culture and treatment with 10 ng/ml of transforming growth factor β 1 (TGF β 1; R&D Systems, Abingdon, UK) in a chemically defined serum-free medium, was performed as described elsewhere (19). Whole-mount staining of the micromasses with Alcian blue at pH 0.2 (0.5% Alcian blue 8 GS [Carl Roth, Karlsruhe, Germany] in 1N HCl) was performed as described previously (19). For quantitation, the Alcian blue-stained micromasses were extracted with 6M guanidine HCl for 6 hours at room temperature. The optical density of the extracted dye was measured at 630 nm.

Transplantation of expanded periosteal cells into a goat model of joint surface defect repair. The joint surface defect in the goat was created as described previously (29). In a first surgical procedure, a joint surface defect was created in the lateral femoral condyle of two 1.5-year-old female saanen goats (*Capra hircus sana*), preserving the mineralized cartilage and the subchondral bone. The size of the defect was 6 mm in diameter and ~0.8 mm in depth. In the same operation, a 1-cm² periosteum sample was harvested from the proximal tibia for cell isolation. Four weeks later, in a second surgical operation, the joint surface defect generated in the previous arthrotomy was sealed incompletely with a periosteal flap obtained from the proximal tibia, leaving an opening for cell

implantation. The periosteal flap was sutured with the cambium layer facing the bed of the defect. Expanded autologous periosteal cell suspensions (10^5 cells/ μ l in PBS) were labeled with PKH26 as described elsewhere (29) and implanted using a blunt 26-gauge needle syringe until the defect was filled (~ 25 – 30 μ l). The defect was then closed with an additional suture point and sealed with fibrin glue (Tissucol, Baxter Healthcare, Thetford, UK). The animals were killed 3 weeks after cell implantation. The operated knees were dissected and processed as described elsewhere (29). Immunostaining for type II collagen was performed as described previously (29).

In vitro osteogenesis. The in vitro osteogenesis assay was performed as described previously (4). As a cell negative control, human dermal fibroblasts were maintained under identical conditions. Alkaline phosphatase activity was determined as described elsewhere (4), using a commercially available kit (Thermo Electron, Waltham, MA). Protein content was determined with the Bradford protein assay (Bio-Rad, Hertfordshire, UK), using bovine serum albumin (Sigma) as standard. Alkaline phosphatase activity was expressed as arbitrary units per microgram of protein content.

To determine calcium contents, cell layers were rinsed twice with PBS and scraped off the dish into 0.5N HCl. The cell layers were extracted by shaking for 4 hours at 4°C and centrifugation at 1,000g for 5 minutes; the supernatant was used for calcium determination using a commercially available kit (Thermo Electron), according to the manufacturer's instructions. Total calcium was calculated from standard solutions and expressed as micrograms per microgram of protein content (determined in parallel dishes). Alizarin red staining of calcium deposits was performed as described previously (4).

In vivo osteogenesis. Five million Pe-MSCs suspended in 50 μ l of growth medium (10^5 cells/ μ l) were seeded into the osteoinductive Collagraft matrix (NeuColl, Campbell, CA) and implanted subcutaneously into nude mice, as described previously (8). The seeding efficiency varied routinely between 40% and 70%. At different time points up to 20 weeks after implantation, the mice were killed and the constructs dissected. The explants were then cut in two, and one half was used for RNA extraction, and the other half was fixed in 4% formaldehyde. Fixed samples were decalcified overnight in Decal (Serva, Amsterdam, The Netherlands), embedded in paraffin, and sectioned at 7 μ m. Immunostaining for human osteocalcin was performed using a guinea pig anti-human osteocalcin antibody (a gift from E. Van Herck, Legendo, Katholieke Universiteit Leuven, Leuven, Belgium) as described previously (8). Immunoreactivity was detected using a peroxidase-conjugated goat anti-guinea pig secondary antibody (Jackson ImmunoResearch, Soham, UK) and 3,3'-diaminobenzidine (Sigma) as a chromogenic substrate. Nuclei were counterstained with hematoxylin.

Total RNA extraction and reverse transcription-PCR (RT-PCR) analysis. Total RNA was isolated using TRIzol (Life Technologies). After DNase treatment, complementary DNA (cDNA) were obtained by reverse transcription of 2 μ g of total RNA (Thermoscript; Life Technologies) using oligo(dT)₂₀ as primer. Semiquantitative PCR was performed as described previously (7). Real-time quantitative PCR was performed with SYBR Green using the Opticon real-time PCR cycler (MJ Research, Waltham, MA). Gene expression of human cells within mouse tissues was evaluated using primers

specific for human cDNA, as described elsewhere (7–9). The sequences of the primers are listed in Table 1. In semiquantitative RT-PCR, when mouse/human chimeric samples were equalized for the expression of human β -actin, control mouse samples with no human cells were normalized to the mouse/human chimeric sample of the series with the highest mouse/human β -actin. In the mouse/human chimeric muscle samples, the molar ratio of human over mouse β -actin messenger RNA was <0.01 , as determined by quantitative RT-PCR (7). Therefore, as shown below, after normalization for human β -actin at 25 cycles, the 18 cycles performed for mouse/human β -actin were optimal to show that the mouse controls contained at least as much cDNA template as the most concentrated of the experimental mouse/human samples, but not sufficient to reach detection levels of β -actin in the human samples.

RESULTS

Growth potential and phenotype of periosteal cells. Periosteal cell cultures were derived as primary cultures from enzymatically released periosteal cell suspensions by selectively attaching to tissue culture plastic. After the first passage and throughout in vitro expansion, periosteal cells appeared microscopically to be a relatively homogeneous population of fibroblast-like cells.

MSCs display a long-term self-renewal capacity. Thus, we first analyzed the growth kinetics of periosteal cells during culture expansion. The growth curves of periosteal cells from donors of various ages were linear up to at least 30 population doublings, with a progressive age-associated decline in their growth rate (Figure 1A). We then determined semiquantitatively the length of the telomeres at passage 7. Despite the population doublings occurring in the first 7 passages and the undetectable telomerase activity (Figure 1B) and regardless of donor age, the telomeres of the periosteal cell populations we tested were long and were comparable with those of an immortalized cell line, which was used as a positive control (Figure 1C).

To evaluate the phenotype of the expanded periosteal cells, we performed fluorescence-activated cell sorting analysis, testing a marker set associated with multipotent MSCs from other tissue sources including bone marrow (2,3,10). CD45, a marker of hematopoietic lineage cells not expressed by MSCs (2), was not detected in any of the donors tested. We detected the expression of CD105, CD166, CD13, CD73, and D7-FIB uniformly in all donors. CD106 and CD146 displayed variable expression between donors, ranging from 2% to 36% for CD146 and from 6% to 59% for CD106 ($n = 4$), with no correlation with donor age. LNGFR and alkaline phosphatase were undetectable in expanded periosteal

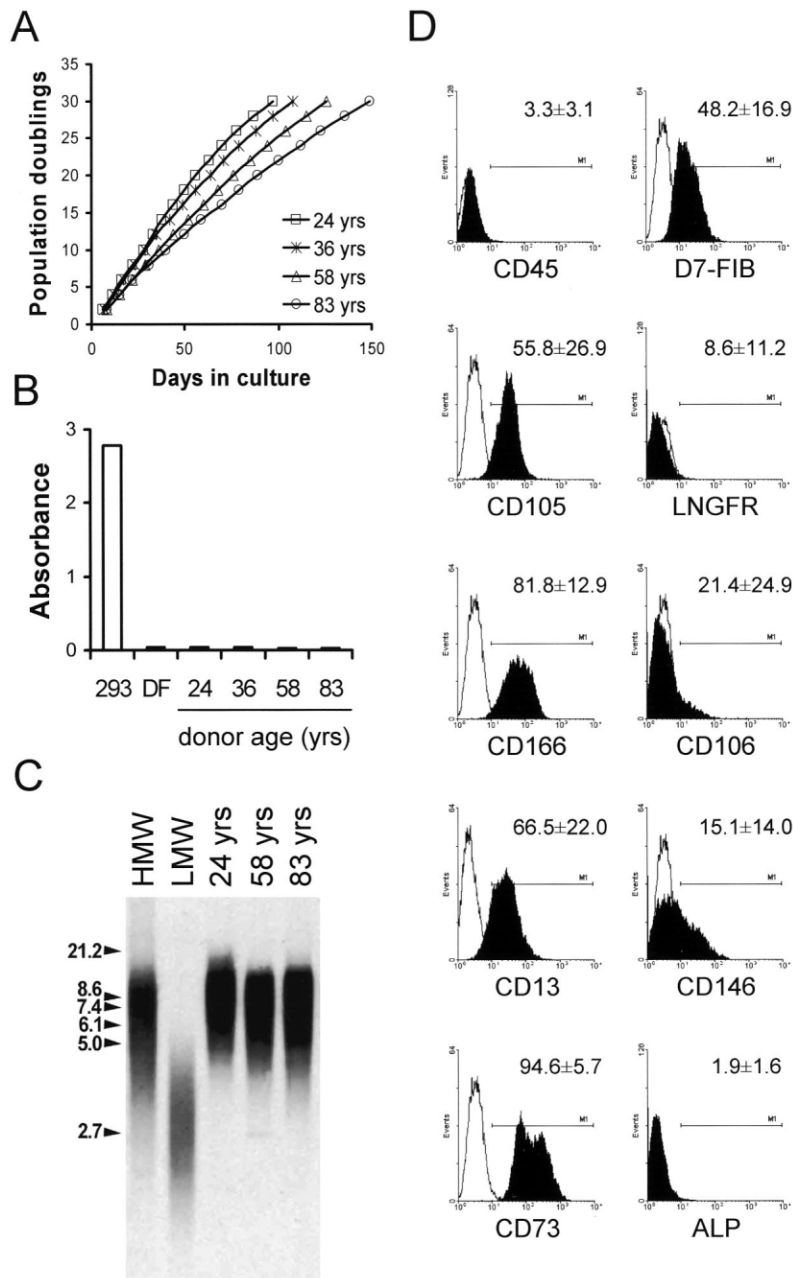


Figure 1. Growth potential and phenotype of periosteal (Pe) mesenchymal stem cells (MSCs). **A**, Kinetics of growth of human Pe-MSCs from 4 donors of different ages, as indicated. Growth kinetics were analyzed starting from the first passage. Cells were plated at 3,000 cells/cm² and expanded in monolayer with serial 1:4 dilution passages upon reaching confluence. The growth curves were linear up to 30 population doublings, with a progressive age-associated decline in the growth rate. **B**, Telomerase activity in passage 5 Pe-MSCs from 4 donors of various ages. Human embryonic kidney 293 cells (293) and human dermal fibroblasts (DF) served as positive and negative controls, respectively. **C**, Southern blotting for telomeres. Expanded human Pe-MSCs from 3 donors of different ages (as indicated) were analyzed by Southern blotting for the length of their telomeres. Regardless of donor age, the telomere lengths were comparable with the U937 cell line that was used as a positive control (high molecular weight [HMW]). HL-60 cells served as a negative control (low molecular weight [LMW]). Molecular weight markers are shown at the left. **D**, Surface marker phenotype of human Pe-MSCs following culture expansion. Results from a representative donor are shown. For each marker tested, the percentage of positive cells is expressed as the mean ± SD of human Pe-MSCs from 4 donors. Solid histograms show marker expression; open histograms show negative isotype controls. Horizontal line shows positive cells.

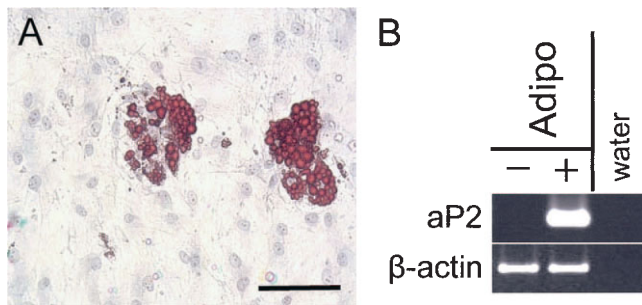


Figure 2. Adipogenic differentiation of periosteal (Pe) mesenchymal stem cells (MSCs). **A**, Oil red O staining of a culture of human Pe-MSCs treated with adipogenic media for 3 weeks. Nuclei were counterstained with hematoxylin. Bar = 50 μ m. **B**, Reverse transcription–polymerase chain reaction analysis of aP2, an adipocyte (Adipo) marker, showing induction upon treatment with adipogenic media. The cDNA were normalized against the expression of the housekeeping gene β -actin. Color figure can be viewed in the online issue, which is available at <http://www.arthritisrheum.org>.

teal cells, as reported with bone marrow MSCs (3). CD73 consistently showed the highest expression levels (mean \pm SD mean fluorescence intensity [MFI] 64 ± 26 units), whereas D7-FIB showed the lowest expression (MFI 11 ± 4 units) (Figure 1D). These data indicate that periosteum contains cells that, upon enzymatic release and culture expansion, display high self-renewal capacity and a phenotype suggestive of multipotent MSCs. Thereafter, we assessed the multipotency toward the mesenchymal lineages.

Adipogenesis of periosteal cells. Adipogenic differentiation was demonstrated by the accumulation of lipid vacuoles and by the expression of the adipocyte marker aP2 (4). In all samples, lipid vacuoles were observed after the first induction treatment and increased in both size and number over time. Such lipid vesicles stained with oil red O (Figure 2A), while untreated cultures were negative (results not shown). The accumulation of lipid vesicles in adipogenic cultures was associated with up-regulation of the adipocyte marker aP2 (Figure 2B). Adipogenic differentiation, as determined by oil red O staining, was achieved in all adipogenic media-treated donor samples tested (results not shown). Four induction treatments resulted in ~ 20 –60% of the cells committing to this lineage, depending on the sample. No apparent correlation was observed with donor age or cell passage number.

Myogenesis of periosteal cells. To investigate the myogenic differentiation of human periosteal cells, we adopted a well-defined *in vivo* mouse model of skeletal muscle regeneration, consisting of injuring the tibialis anterior muscle by the injection of cardiotoxin (7).

Twenty-four hours later, culture-expanded human Pe-MSCs were injected into the same tibialis anterior muscle. To avoid rejection of the human cells, nude mice were used.

We first investigated the integration of human cells into muscle fibers by implanting into regenerating tibialis anterior muscles human periosteal cells transduced with AdCMVLacZ. At 3 weeks, some myofibers displayed diffuse β -galactosidase (β -gal) expression (Figure 3A), demonstrating incorporation of at least 1 transduced human cell for each β -gal–positive fiber. To determine whether the human cells implanted in the mouse tibialis anterior muscles acquired the skeletal muscle phenotype, we used RT-PCR with primers specific for human cDNA. At 4 weeks, we detected human myosin heavy chain type IIx/d (MyHC-IIx/d) in the tibialis anterior muscles injected with human Pe-MSCs (Figure 3B). Myogenic differentiation, as determined by RT-PCR for human MyHC-IIx/d, was achieved in all donor samples tested (results not shown). Together, these data indicate that expanded human periosteal cells have the capacity to undergo skeletal myogenesis *in vivo*, contributing to muscle regeneration.

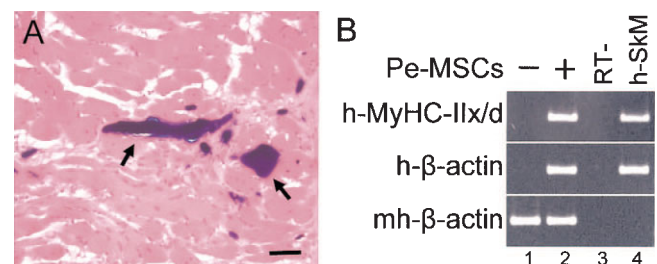


Figure 3. Skeletal muscle differentiation of periosteal (Pe) mesenchymal stem cells (MSCs). **A**, X-Gal staining with hematoxylin and eosin counterstaining at 3 weeks after transplantation of human Pe-MSCs transduced with adenovirus cytomagalovirus promoter LacZ protein. **Arrows** indicate muscle fibers with diffuse β -galactosidase expression, indicating incorporation of transduced human cells. Bar = 50 μ m. **B**, Semiquantitative reverse transcription–polymerase chain reaction analysis of human myosin heavy chain type IIx/d (h-MyHC-IIx/d). At 4 weeks after transplantation, human MyHC-IIx/d was detected in the muscle injected with Pe-MSCs. Lane 1, Cardiotoxin-treated muscle injected with phosphate buffered saline (tissue-negative control); lane 2, cardiotoxin-treated tibialis anterior muscle injected with human Pe-MSCs; lane 3, reverse transcriptase–negative (RT–) control of lane 2; lane 4, human skeletal muscle (h-SkM; positive control). The cDNA were normalized against the expression of human β -actin (h- β -actin). mh indicates that the primer set did not allow a distinction between mouse and human cDNA. Color figure can be viewed in the online issue, which is available at <http://www.arthritisrheum.org>.

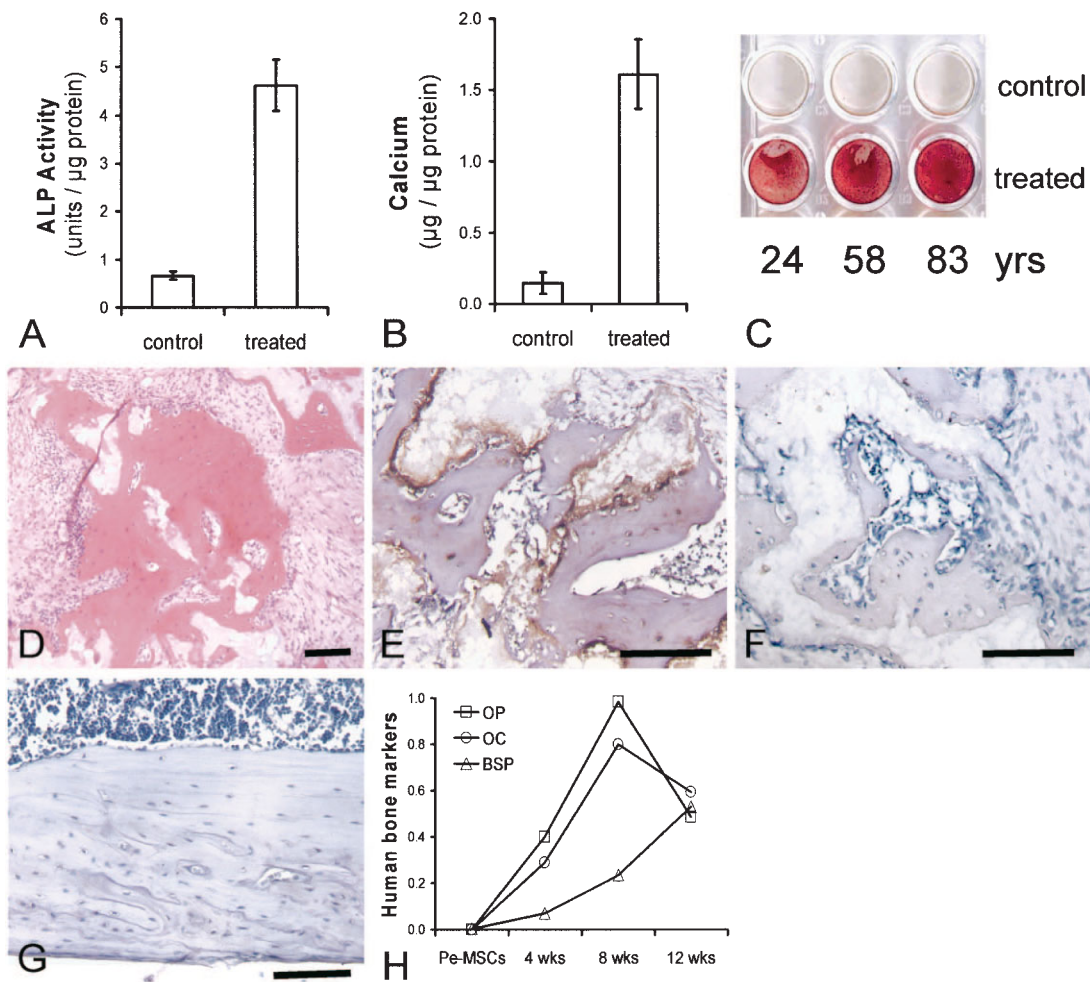


Figure 4. Osteogenic differentiation of periosteal (Pe) mesenchymal stem cells (MSCs). **A–C**, In vitro osteogenesis. **A**, Alkaline phosphatase (ALP) activity at 8 days of treatment with osteogenic medium (expressed as arbitrary units per microgram of protein content). **B**, Calcium deposition of human Pe-MSCs at 3 weeks of treatment (expressed as microgram of calcium per microgram of protein content, determined in parallel wells). Values in **A** and **B** are the mean \pm SD of human Pe-MSCs from 4 donors. **C**, Alizarin red staining at 3 weeks in 3 representative donors of different ages, as indicated. **D–H**, In vivo bone formation. Human Pe-MSCs were seeded into Collagraft scaffolds, and the constructs were implanted subcutaneously into nude mice. **D**, Hematoxylin and eosin staining at 20 weeks after implantation. **E–G**, Immunohistochemistry for human osteocalcin, showing Collagraft scaffold seeded with human Pe-MSCs at 8 weeks after implantation (**E**), isotype-negative control for **E** (**F**), and mouse bone as a tissue-negative control (**G**). Nuclei were counterstained with hematoxylin. Bars in **D–G** = 100 μ m. **H**, Gene expression dynamics during bone formation in vivo. Expression of the bone markers osteocalcin (OC), osteopontin (OP), and bone sialoprotein (BSP), normalized against human β -actin, was monitored by quantitative reverse transcription–polymerase chain reaction analysis in Pe-MSC monolayers and at 4, 8, and 12 weeks after implantation of the Collagraft constructs. The primers used were specific for the human genes. The bone markers, which were barely detectable in the monolayer cultures, were up-regulated in vivo.

Osteogenesis of periosteal cells. Periosteal cells treated with osteogenic medium formed large nodules that stained positive for alkaline phosphatase and with alizarin red (results not shown). This process was associated with a significant increase in alkaline phosphatase

activity at 8 days (Figure 4A) and calcium deposits at 3 weeks (Figure 4B). Osteogenic differentiation, as determined by alizarin red staining, was achieved in all osteogenic medium–treated donor samples tested (representative samples shown in Figure 4C). Calcium de-

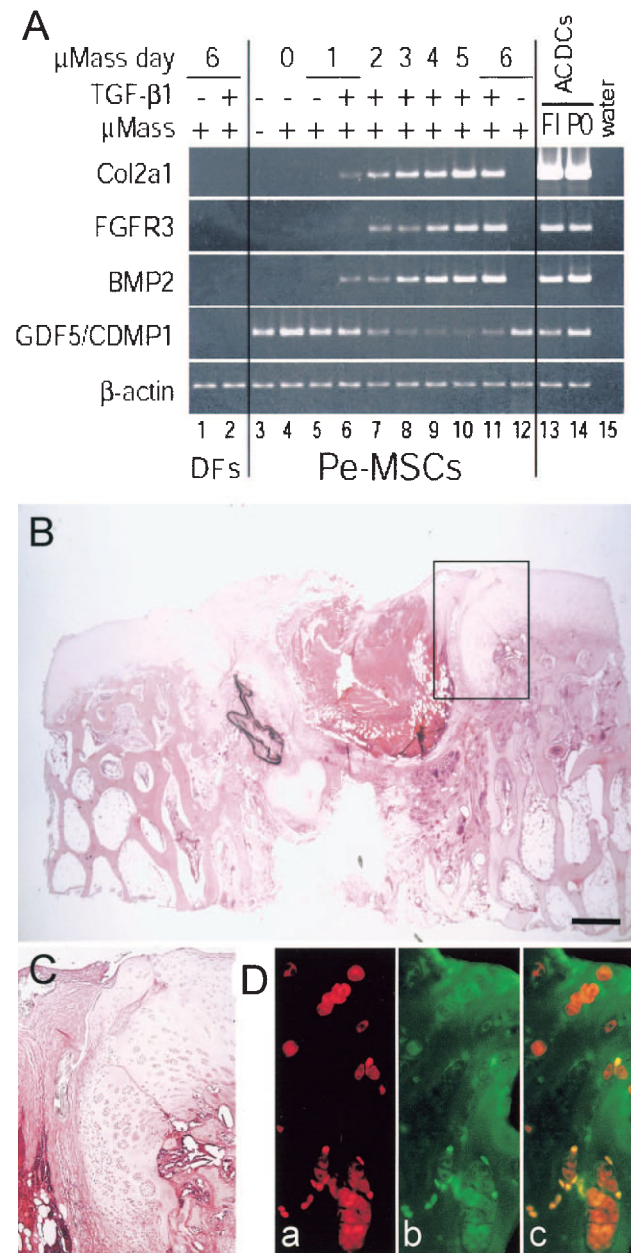


Figure 5. Chondrogenic differentiation of periosteal (Pe) mesenchymal stem cells (MSCs). **A**, Dynamics of gene expression during the early phase of chondrogenesis in transforming growth factor $\beta 1$ (TGF $\beta 1$)-treated Pe-MSC micromasses in vitro, as determined by semiquantitative reverse transcription–polymerase chain reaction analysis. Lanes 1 and 2, Human dermal fibroblasts (DFs) in micromass (μ Mass); lane 3, human Pe-MSCs in monolayer; lanes 4–12, human Pe-MSCs in micromass; lanes 13 and 14, freshly isolated (FI) and passage 0 (P0) adult human articular cartilage–derived cells (ACDCs). The down-regulation of the early chondrocyte–lineage marker growth differentiation factor 5 (GDF-5)/cartilage-derived morphogenetic protein 1 (CDMP-1) was associated with a progressive increase in the expression levels of bone morphogenetic protein 2 (BMP-2), fibroblast growth factor receptor 3 (FGFR-3), and type II collagen (Col2a1) over time. **B–D**, In vivo cartilage formation by Pe-MSCs in a goat model of joint surface defect repair. Expanded autologous goat Pe-MSCs were fluorescence-labeled with PKH26 (red) and implanted into a joint surface defect under a periosteal flap in the goat. **B**, Hematoxylin and eosin staining at 3 weeks. There was no repair with delamination of the periosteal flap. Cartilage, probably partly newly formed, was visible at the margins of the defect (boxed area), as shown at higher magnification in **C**. Bar = 1 mm. **D**, Persistence and chondrogenic differentiation of Pe-MSCs in the boxed area shown in **A** and shown at higher magnification in **C**. **a**, Red fluorescent image showing persistence of the implanted PKH26-labeled Pe-MSCs. **b**, Green fluorescent image showing type II collagen immunostaining. **c**, Superimposition of the red fluorescent image indicating the labeled implanted cells and the green fluorescent image showing immunofluorescence detection of type II collagen.

posits were not detected in control periosteal cell cultures or in skin fibroblasts treated with osteogenic medium, which were used as a cell negative control (results not shown).

To investigate whether periosteal cells can form bone *in vivo*, we adopted a validated assay for bone formation, which consists of seeding the cells into osteoinductive Collagraft scaffolds and implanting the constructs under the skin of immunodeficient nude mice (8). Starting from 8 weeks after implantation, areas of bone were observed on hematoxylin and eosin-stained sections (Figure 4D). To investigate the human origin of the bone tissue, we performed immunostaining using an antibody specific for human osteocalcin (Figures 4E, F, and G). Mouse bone was used to control the human specificity of the antibody (Figure 4G). Areas that morphologically appeared to be bone stained positive for human osteocalcin (Figure 4E), demonstrating a contribution of human cells to bone formation. Conversely, no bone could be retrieved when empty Collagraft or Collagraft seeded with expanded dermal fibroblasts was used in parallel experiments (results not shown).

To confirm differentiation of the human Pe-MSCs into an osteoblast phenotype at the molecular level, we monitored gene expression by real-time quantitative RT-PCR using human-specific primers. The bone markers osteopontin, osteocalcin, and bone sialoprotein, which were barely detectable in the monolayer cultures, were progressively up-regulated in the periosteal cell-Collagraft implants over time (Figure 4H). Mouse bone was used to ensure specificity of the primers for human cDNA (results not shown). Chondrocyte markers such as types II, IX, and X collagen were undetectable at the time points examined (results not shown).

Chondrogenesis of periosteal cells. In studies combining micromass culture and TGF β 1 treatment in a chemically defined serum-free medium, we previously demonstrated that periosteal cells display chondrogenic potential *in vitro* (19). In a time-point analysis using this *in vitro* assay, we observed that early chondrogenesis was associated with a cascade of molecular events (Figure 5A), which is reminiscent of embryonic chondrogenesis (30). In particular, down-regulation of the early chondrocyte lineage marker growth differentiation factor 5/cartilage-derived morphogenetic protein 1 (31) was associated with a progressive increase in the expression levels of bone morphogenetic protein 2, fibroblast growth factor receptor 3, and type II collagen over time (Figure 5A).

To investigate the chondrogenic potential *in vivo*, we implanted PKH26-labeled expanded autologous periosteal cells in an experimental joint surface defect under a periosteal flap in goats (29). The labeling did not affect the differentiation potential of the cells *in vitro* (results not shown). At 3 weeks after implantation, there was no repair, with delamination of the periosteal flap. Instead, the defect was enlarged and filled with a fibrous-like tissue (Figure 5B), possibly because of extensive subchondral bone remodeling, as reported previously (32). However, cartilage tissue was evident histologically at the margins of the defect (Figure 5C). In this area, we detected clusters of cells displaying double fluorescence for PKH26 and type II collagen (Figure 5D). Thus, this experiment provides proof of concept that a proportion of the implanted periosteal cells can undergo chondrogenesis *in vivo*.

Multipotency inherent at the single-cell level.

The phenotype analysis (Figure 1D) showed that expanded Pe-MSCs populations are heterogeneous for some of the markers tested. We therefore investigated whether individual periosteal cells can give rise to multiple differentiated phenotypes or whether each phenotype arises from a subset of committed progenitor cells that exists within a heterogeneous population. To this end, first-passage periosteal cells from 4 donors were subjected to classic limiting dilution, yielding 7 expandable single-cell-derived clones. The telomere lengths, telomerase activity, and marker profile of the expanded clonal populations were similar to those of the parental Pe-MSCs populations (results not shown). After 22–24 population doublings, and still in the linear phase of their growth curves, the clonal populations were assessed for their potential to undergo chondrogenesis, osteogenesis, and adipogenesis *in vitro* and myogenesis *in vivo*. Under our experimental conditions, all clones displayed multipotency for the mesenchymal lineages tested (Figure 6).

DISCUSSION

Periosteum contains cells that, upon enzymatic release and culture expansion, can give rise to cartilage and bone (13–21,23–26) as well as to adipocytes, as recently reported (22). This potential can be due to functionally distinct progenitor cells or to a common primitive stem cell with inherent multipotentiality, with the two hypotheses being not mutually exclusive. We present herein evidence that cells derived from the periosteum of adult humans, regardless of donor age, possess high self-renewal capacity, express a marker set

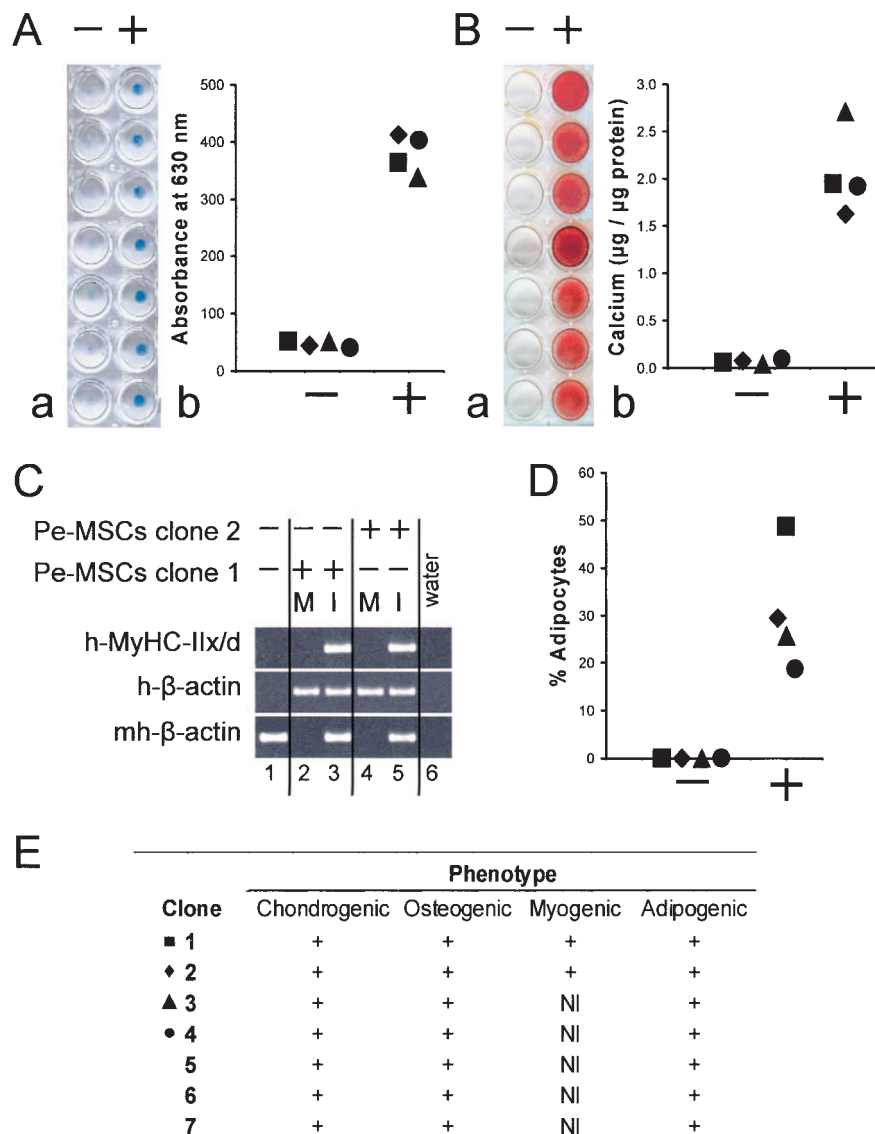


Figure 6. Multipotency of periosteal single-cell-derived clonal populations. Single-cell-derived clonal populations were prepared by limiting dilution, expanded in culture, and in the linear phase of their growth curves, subjected to differentiation assays. **A**, Chondrogenic differentiation. Cells were plated in micromass culture and were either treated (+) or not treated (-) with transforming growth factor $\beta 1$ (TGF $\beta 1$) for 6 days. **a**, Alcian blue staining. **b**, Stained micromasses of 4 clones were extracted with 6M guanidine HCl, and the absorbance of the extracted dye was measured at 630 nm. No difference was detected in DNA and protein contents between TGF $\beta 1$ -treated and control micromasses (results not shown). **B**, Osteogenic differentiation. Clonal cell populations in monolayers were either treated or not treated with osteogenic medium for 3 weeks. **a**, Alizarin red staining. **b**, Quantitation of calcium deposition in 4 clones (expressed as microgram of calcium per microgram of protein content, determined in parallel wells). **C**, Myogenic differentiation. Two periosteal clones were assessed for their myogenic potential by injecting them into regenerating nude mouse tibialis anterior muscles. Semiquantitative reverse transcription-polymerase chain reaction for human myosin heavy chain type IIx/d (h-MyHC-IIx/d) at 4 weeks. The cDNA were normalized against the expression of human β -actin (h- β -actin). Human MyHC-IIx/d was detected in both tibialis anterior muscles injected (I) with either of the 2 clonal cell populations tested (lanes 3 and 5). Human MyHC-IIx/d was not expressed at detectable levels by Pe-MSC clones in monolayer (M) before implantation (lanes 2 and 4). Lane 1, Mouse cardiotoxin-treated tibialis anterior. mh indicates that the primer set did not allow a distinction between mouse and human cDNA. **D**, Adipogenic differentiation. Shown are the percentages of oil red O-stained cells of 4 clonal populations either treated or not treated with adipogenic media. **E**, The multilineage differentiation potential of the clonal populations tested. NI = not investigated. The 4 different symbols indicate the 4 clones shown in **Aa**, **Bb**, and **D**. Color figure can be viewed in the online issue, which is available at <http://www.arthritisrheum.org>.

of MSCs, and display mesenchymal multipotency at the single-cell level since they can differentiate toward chondrogenesis, osteogenesis, adipogenesis, and skeletal myogenesis *in vitro* and *in vivo*. Thus, our findings extend to human periosteum the accessibility to tissue sources of multipotent MSCs for clinical application in tissue engineering and regenerative medicine. A small periosteal biopsy represents a relatively easily accessible source of MSCs. We have shown a context-sensitive and site-specific differentiation response of Pe-MSCs, which suggests a low risk of heterotopic tissue formation in clinical applications. However, this remains to be tested in appropriate animal models.

Our data showing multipotency at the single periosteal cell level are not necessarily at odds with those of a previous clonal study using freshly isolated chick periosteal cells in an agar gel culture system that suggested the presence of distinct chondroprogenitors and osteoprogenitors in the periosteal cell population (27). This apparent discrepancy could be explained by the different experimental systems used. Indeed, with our experimental design, we cannot rule out dedifferentiation of chondro-osteogenic progenitors resulting in a population of multipotent MSCs, nor can we exclude the possibility that functionally distinct progenitors might coexist in the periosteal cell population, with our culture conditions favoring the more primitive multipotent MSC population. Yet, our phenotype analysis showed that expanded Pe-MSC populations are not homogeneous for the markers tested. This phenotypic heterogeneity of Pe-MSCs could be due to the coexistence of multiple distinct cell types, as reported with bone marrow MSCs (33,34), or it could reflect functional heterogeneity of the same cell type, as reported with osteoprogenitor clones (35). We favor the second hypothesis, since a similar heterogeneity was observed in the expanded multipotent single-cell-derived clonal populations.

Despite the remarkable self-renewal capacity of Pe-MSCs, the activity of telomerase, a ribonucleoprotein polymerase that regulates the cell's proliferative lifespan (36), was not detected under our experimental conditions. Telomere elongation by telomerase is thought to be necessary to guarantee a high number of cell divisions (36). Nonetheless, Pe-MSCs maintained linear growth curves over at least 30 population doublings. This high self-renewal capacity might be attributable to the length of telomeres in periosteal cell populations, which would counterbalance the undetectable telomerase activity (37). Telomerase-independent mechanisms that preserve the telomere length have also been postulated (36). Alternatively, a small subpopula-

tion of cells possessing significant telomerase activity could be responsible for the self-renewal capacity. This, however, appears to be unlikely, since telomerase activity was not detected in any of the clonal populations.

We provide proof of concept that expanded periosteal cells can form cartilage *in vivo* when implanted into a joint surface defect in a goat model. Long-term studies in animal models of joint surface defect repair (29) are necessary to evaluate the potential use of Pe-MSCs in joint resurfacing, their phenotypic behavior within the articular cartilage microenvironment, and in particular, whether the cartilage contributed by the implanted periosteal cells remains stable or is a transient tissue that is destined to be replaced by bone.

The bone tissue retrieved *in vivo* was at least partly of human origin. We cannot exclude a contribution of mouse host cells to bone formation, and this is presently under investigation. However, under our experimental conditions, human Pe-MSCs were necessary, since no bone could be retrieved when empty Collagraft or Collagraft seeded with expanded dermal fibroblasts was used in parallel experiments. The retrieved bone appears to have formed directly through membranous ossification, since we did not detect cartilage tissue by histology or expression of chondrocyte markers such as type II collagen by RT-PCR at the time points examined.

This is the first report showing that cells derived from the adult human periosteum can also differentiate into skeletal muscle *in vivo* and are multipotent MSCs at the single-cell level. Multipotency could be the result of the disruption of a mechanism of differentiation control caused by the *ex vivo* cell manipulations. Alternatively, multipotency could be an intrinsic property of reserve quiescent cells that reside within the adult periosteum and undergo activation in response to signals from the surrounding tissue/structures. This is suggested by the role of perichondrium during embryonic skeletogenesis and of periosteum in adult life. During embryonic development, the perichondrium, which is called periosteum after ossification, provides cells that are recruited for the growth of the developing skeletal elements (38). In postnatal life, the periosteum is involved in physiologic bone appositional growth and remodeling and is necessary for fracture healing, contributing cells to callus formation and endochondral ossification (39). Since it has been shown that fetal perichondrial cells are multipotent toward mesenchymal lineages (40), it is tempting to speculate that undifferentiated multipotent

MSCs could persist in the periosteum in adult life. Compelling evidence is awaited.

Like MSCs derived from bone marrow, trabecular bone, synovial membrane, synovial fluid, or adipose tissue (1–4,6,7,9,10,41), Pe-MSCs rapidly adhere to plastic and can be expanded for several passages, preserving their multipotency. Whether Pe-MSCs are resident “static” cells or are part of a common pool of “dynamic” MSCs that could travel through circulation from one tissue to another is debatable. Circulating MSCs have been identified (42). Nonetheless, the derivation of Pe-MSCs from circulating MSC populations would not exclude the possibility that by residing in the periosteum, MSCs could acquire distinctive biologic properties. Increasing evidence suggests that MSCs isolated from different tissues and organs have distinctive features *in vitro* and *in vivo* (22,42–45). The variability in the biologic properties of MSC populations is likely to affect the outcome of clinical applications. At the same time, the availability of several MSC populations with distinct differentiation properties is desirable because it allows a broader choice in the optimization of different tissue repair protocols.

Systematic quantitative studies comparing adult human MSCs derived from different tissues are therefore desirable. Such studies would identify specific indications for different MSCs and, in particular, the optimal MSC populations for the biologic repair of each individual skeletal tissue. Additionally, the studies would satisfy the need to establish MSC populations with consistent and reproducible biologic behaviors, quality-controlled for specific therapeutic applications (46,47).

ACKNOWLEDGMENTS

We thank the orthopedic surgeons of the Katholieke Universiteit Leuven and Guy's Hospital London for providing periosteal samples. Special thanks are due to the staff of the mortuary at the University Hospitals Katholieke Universiteit Leuven. We are also grateful to TiGenix (Leuven, Belgium) for providing technologies required for the goat experiment.

REFERENCES

- Prockop DJ. Marrow stromal cells as stem cells for nonhematopoietic tissues. *Science* 1997;276:71–4.
- Pittenger MF, Mackay AM, Beck SC, Jaiswal RK, Douglas R, Mosca JD, et al. Multilineage potential of adult human mesenchymal stem cells. *Science* 1999;284:143–7.
- Jones EA, Kinsey SE, English A, Jones RA, Straszynski L, Meredith DM, et al. Isolation and characterization of bone marrow multipotential mesenchymal progenitor cells. *Arthritis Rheum* 2002;46:3349–60.
- De Bari C, Dell'Accio F, Tylzanowski P, Luyten FP. Multipotent mesenchymal stem cells from adult human synovial membrane. *Arthritis Rheum* 2001;44:1928–42.
- Asakura A, Komaki M, Rudnicki M. Muscle satellite cells are multipotential stem cells that exhibit myogenic, osteogenic, and adipogenic differentiation. *Differentiation* 2001;68:245–53.
- Zuk PA, Zhu M, Mizuno H, Huang J, Futrell JW, Katz AJ, et al. Multilineage cells from human adipose tissue: implications for cell-based therapies. *Tissue Eng* 2001;7:211–28.
- De Bari C, Dell'Accio F, Vandenabeele F, Vermeesch JR, Raymackers JM, Luyten FP. Skeletal muscle repair by adult human mesenchymal stem cells from synovial membrane. *J Cell Biol* 2003;160:909–18.
- Dell'Accio F, De Bari C, Luyten FP. Microenvironment and phenotypic stability specify tissue formation by human articular cartilage-derived cells *in vivo*. *Exp Cell Res* 2003;287:16–27.
- De Bari C, Dell'Accio F, Luyten FP. Failure of *in vitro*-differentiated mesenchymal stem cells from the synovial membrane to form ectopic stable cartilage *in vivo*. *Arthritis Rheum* 2004;50:142–50.
- Jones EA, English A, Henshaw K, Kinsey SE, Markham AF, Emery P, et al. Enumeration and phenotypic characterization of synovial fluid multipotential mesenchymal progenitor cells in inflammatory and degenerative arthritis. *Arthritis Rheum* 2004;50:817–27.
- Alsalameh S, Amin R, Gemba T, Lotz M. Identification of mesenchymal progenitor cells in normal and osteoarthritic human articular cartilage. *Arthritis Rheum* 2004;50:1522–32.
- Dowthwaite GP, Bishop JC, Redman SN, Khan IM, Rooney P, Evans DJ, et al. The surface of articular cartilage contains a progenitor cell population. *J Cell Sci* 2004;117:889–97.
- Nakahara H, Bruder SP, Goldberg VM, Caplan AI. *In vivo* osteochondrogenic potential of cultured cells derived from the periosteum. *Clin Orthop* 1990;259:223–32.
- Nakahara H, Bruder SP, Haynesworth SE, Holecek JJ, Baber MA, Goldberg VM, et al. Bone and cartilage formation in diffusion chambers by subcultured cells derived from the periosteum. *Bone* 1990;11:181–8.
- Nakahara H, Goldberg VM, Caplan AI. Culture-expanded human periosteal-derived cells exhibit osteochondral potential *in vivo*. *J Orthop Res* 1991;9:465–76.
- Izumi T, Scully SP, Heydemann A, Bolander ME. Transforming growth factor β 1 stimulates type II collagen expression in cultured periosteum-derived cells. *J Bone Miner Res* 1992;7:115–21.
- Iwasaki M, Nakata K, Nakahara H, Nakase T, Kimura T, Kimata K, et al. Transforming growth factor- β 1 stimulates chondrogenesis and inhibits osteogenesis in high density culture of periosteum-derived cells. *Endocrinology* 1993;132:1603–8.
- Iwasaki M, Nakahara H, Nakase T, Kimura T, Takaoka K, Caplan AI, et al. Bone morphogenetic protein 2 stimulates osteogenesis but does not affect chondrogenesis in osteochondrogenic differentiation of periosteum-derived cells. *J Bone Miner Res* 1994;9:1195–204.
- De Bari C, Dell'Accio F, Luyten FP. Human periosteum-derived cells maintain phenotypic stability and chondrogenic potential throughout expansion regardless of donor age. *Arthritis Rheum* 2001;44:85–95.
- Gruber R, Mayer C, Bobacz K, Krauth MT, Graninger W, Luyten FP, et al. Effects of cartilage-derived morphogenetic proteins and osteogenic protein-1 on osteochondrogenic differentiation of periosteum-derived cells. *Endocrinology* 2001;142:2087–94.
- Hanada K, Solchaga LA, Caplan AI, Hering TM, Goldberg VM, Yoo JU, et al. BMP-2 induction and TGF- β 1 modulation of rat periosteal cell chondrogenesis. *J Cell Biochem* 2001;81:284–94.
- Sakaguchi Y, Sekiya I, Yagishita K, Muneta T. Comparison of human stem cells derived from various mesenchymal tissues: superiority of synovium as a cell source. *Arthritis Rheum* 2005;52:2521–9.

23. Breitbart AS, Grande DA, Kessler R, Ryaby JT, Fitzsimmons RJ, Grant RT. Tissue engineered bone repair of calvarial defects using cultured periosteal cells. *Plast Reconstr Surg* 1998;101:567-74.
24. Vacanti CA, Bonassar LJ, Vacanti MP, Shufflebarger J. Replacement of an avulsed phalanx with tissue-engineered bone. *N Engl J Med* 2001;344:1511-4.
25. Grande DA, Mason J, Light E, Dines D. Stem cells as platforms for delivery of genes to enhance cartilage repair. *J Bone Joint Surg Am* 2003;85-A Suppl 2:111-6.
26. Hutmacher DW, Sittlinger M. Periosteal cells in bone tissue engineering. *Tissue Eng* 2003;9 Suppl 1:S45-64.
27. Nakase T, Nakahara H, Iwasaki M, Kimura T, Kimata K, Watanabe K, et al. Clonal analysis for developmental potential of chick periosteum-derived cells: agar gel culture system. *Biochem Biophys Res Commun* 1993;195:1422-8.
28. Taswell C. Limiting dilution assays for the determination of immunocompetent cell frequencies. I. Data analysis. *J Immunol* 1981;126:1614-9.
29. Dell'Accio F, Vanlauwe J, Bellemans J, Neys J, De Bari C, Luyten FP. Expanded phenotypically stable chondrocytes persist in the repair tissue and contribute to cartilage matrix formation and structural integration in a goat model of autologous chondrocyte implantation. *J Orthop Res* 2003;21:123-31.
30. Dell'Accio F, De Bari C, Luyten FP. Molecular basis of joint development. *Jpn J Rheumatol* 1999;9:17-29.
31. Luyten FP, Lories R, De Valck D, De Bari C, Dell'Accio F. Bone morphogenetic proteins and the synovial joints. In: Vukicevic S, Sampath KT, editors. *Progress in inflammation research*. Basel: Birkhauser Verlag; 2002. p. 223-48.
32. Vasara AI, Hyttinen MM, Lammi MJ, Lammi PE, Langsjö TK, Lindahl A, et al. Subchondral bone reaction associated with chondral defect and attempted cartilage repair in goats. *Calcif Tissue Int* 2004;74:107-14.
33. Muraglia A, Cancedda R, Quarto R. Clonal mesenchymal progenitors from human bone marrow differentiate in vitro according to a hierarchical model. *J Cell Sci* 2000;113:1161-6.
34. Okamoto T, Aoyama T, Nakayama T, Nakamata T, Hosaka T, Nishijo K, et al. Clonal heterogeneity in differentiation potential of immortalized human mesenchymal stem cells. *Biochem Biophys Res Commun* 2002;295:354-61.
35. Madras N, Gibbs AL, Zhou Y, Zandstra PW, Aubin JE. Modeling stem cell development by retrospective analysis of gene expression profiles in single progenitor-derived colonies. *Stem Cells* 2002;20:230-40.
36. Blasco MA, Gasser SM, Lingner J. Telomeres and telomerase. *Genes Dev* 1999;13:2353-9.
37. Bodnar AG, Ouellette M, Frolkis M, Holt SE, Chiu CP, Morin GB, et al. Extension of life-span by introduction of telomerase into normal human cells. *Science* 1998;279:349-52.
38. Tsumaki N, Tanaka K, Arikawa HE, Nakase T, Kimura T, Thomas JT, et al. Role of CDMP-1 in skeletal morphogenesis: promotion of mesenchymal cell recruitment and chondrocyte differentiation. *J Cell Biol* 1999;144:161-73.
39. Orwoll ES. Toward an expanded understanding of the role of the periosteum in skeletal health. *J Bone Miner Res* 2003;18:949-54.
40. Arai F, Ohneda O, Miyamoto T, Zhang XQ, Suda T. Mesenchymal stem cells in perichondrium express activated leukocyte cell adhesion molecule and participate in bone marrow formation. *J Exp Med* 2002;195:1549-63.
41. Tuli R, Tuli S, Nandi S, Wang ML, Alexander PG, Haleem-Smith H, et al. Characterization of multipotential mesenchymal progenitor cells derived from human trabecular bone. *Stem Cells* 2003;21:681-93.
42. Kuznetsov SA, Mankani MH, Gronthos S, Satomura K, Bianco P, Robey PG. Circulating skeletal stem cells. *J Cell Biol* 2001;153:1133-40.
43. Batouli S, Miura M, Brahim J, Tsutsui TW, Fisher LW, Gronthos S, et al. Comparison of stem-cell-mediated osteogenesis and dentinogenesis. *J Dent Res* 2003;82:976-81.
44. Hui JH, Li L, Teo YH, Ouyang HW, Lee EH. Comparative study of the ability of mesenchymal stem cells derived from bone marrow, periosteum, and adipose tissue in treatment of partial growth arrest in rabbit. *Tissue Eng* 2005;11:904-12.
45. Matsubara T, Suardita K, Ishii M, Sugiyama M, Igarashi A, Oda R, et al. Alveolar bone marrow as a cell source for regenerative medicine: differences between alveolar and iliac bone marrow stromal cells. *J Bone Miner Res* 2005;20:399-409.
46. Luyten FP, De Bari C, Dell'Accio F. Identification and characterization of human cell populations capable of forming stable hyaline cartilage in vivo. In: Hascall VC, Kuettner KE, editors. *The many faces of osteoarthritis*. Basel: Birkhauser Verlag; 2002. p. 67-76.
47. Luyten FP, Dell'Accio F, De Bari C. Skeletal tissue engineering: opportunities and challenges. *Best Pract Res Clin Rheumatol* 2001;15:759-69.